Hemodynamic Environment Characteristics in the Ascending Aorta After Dilation Formed for the Bicuspid Aortic Valve Patients

Tie Zheng
Beijing An Zhen Hospital: Capital Medical University Affiliated Anzhen Hospital
Shuai Zhu
Beijing Luhe Hospital
Shijie Lu
Beijing An Zhen Hospital: Capital Medical University Affiliated Anzhen Hospital
Jiafu Ou
Washington University
Jun-Ming Zhu (anzhenzjm@163.com)
Department of Cardiovascular Surgery, Beijing Aortic Disease Center, Beijing Anzhen Hospital, Capital Medical University, Beijing, China; Beijing Institute of Heart Lung and Blood Vessel Diseases, Beijing 100029, China https://orcid.org/0000-0002-6919-9164

Research

Keywords: Bicuspid aortic valve, Hemodynamics, Aortic dilation, Aorta

Posted Date: October 29th, 2020

DOI: https://doi.org/10.21203/rs.3.rs-97685/v1

Title：Hemodynamic environment characteristics in the ascending aorta after dilation formed for the bicuspid aortic valve patients

Tie Zheng[a], Shuai Zhu[b], Shijie Lu[a], Jiafu Ou[b], Junming Zhu[a*],

a Department of Cardiovascular Surgery, Beijing Aortic Disease Center, Beijing Anzhen Hospital, Capital Medical University, Beijing, China; Beijing Institute of Heart Lung and Blood Vessel Diseases, Beijing 100029, China

b Beijing Luhe Hospital, Capital Medical University, Beijing 101149, China;

b Cardiology Division, Department of Internal Medicine, Washington University in St. Louis, 63110 USA

Tie Zheng [a]： tiezheng@aliyun.com

*Corresponding authors:

Junming Zhu[a]: anzhenzjm@163.com

Fax: +86 10 64456595

Abstract

Background: The bicuspid aortic valve is one of the common congenital heart anomalies in adults. Although many studies have proved the coincidence between bicuspid aortic valve and the occurrence of ascending aortic dilation, seldom study has focused on the hemodynamic environments after the dilation already formed. Four numerical models of bicuspid aortic valve were constructed in this study, based on medical images, with different ascending aortic dilation levels. The diameters of ascending aortic are 3.5cm, 4.0cm, 4.5cm and 5.0cm, respectively; while, the size and the geometry of other parts are fixed. Then hemodynamics in these models was simulated numerically and the flow patterns and loading distributions were investigated. Aim of this study is to investigate the hemodynamic environment characteristics in the ascending aorta after dilation formed for the bicuspid aortic valve (BAV) patients.

Results: Hemodynamics environments in the dilated ascending aorta were simulated, with different level of dilation. As the diameter increases, the blood flow becomes more disturbing. The wall shear stress at the ascending aortic decreases while oscillatory shear index increases with the increase of diameter. The pressure at ascending aortic increases as the diameter increases. Moreover, all these hemodynamic parameters described above are asymmetrically distributed with the increase of ascending aortic diameter and more parts of aorta would be affected with the increasing ascending aorta diameters

Conclusions: The study revealed that the ascending aortic dilation levels can significantly influence the magnificent and distribution of the dynamics. There are altered flow patterns, pressure difference, WSS and OSI distribution features in bicuspid aortic valve patients with valvular dilation. As the extent of aortic dilatation increases, more parts of aorta like aortic arch should be paid more attention to when an individual is referred for surgery

Key words: Bicuspid aortic valve, Hemodynamics, Aortic dilation, Aorta

Background

The bicuspid aortic valve (BAV) is one of the common congenital heart anomalies in adults. BAV is an inherited form of heart disease in which two of the leaflets of the aortic valve fuse during fetal development resulting in a two-leaflet valve (bicuspid valve) instead of the normal three-leaflet valve (trileaflet valve).

Previous studies have revealed that the BAV will disturb the physiological flow patterns perfuse to the ascending aorta and cause the hemodynamic environment there abnormal(1, 2). Previous studies found that for BAV patients, the wall shear stress (WSS) distribution at the ascending aorta expressed in a high and very asymmetric way(3, 4). Many studies(5-8) reported that the abnormal pulsatile flow patterns of BAV patients has effects on the endothelial cells of the arterial wall, and then activate the remodeling process of artery wall. One of the severe consequences is the dilatation of ascending aorta, which would finally induce ascending aortic aneurysm or aortic dissection.

Although many studies have proved the coincidence between BAV and the occurrence of ascending aortic dilation(1, 9, 10), seldom study has focused on the hemodynamic environments after the dilation already formed. We think that it is also very essential to investigate and present the hemodynamic environments in different dilation stages of ascending aorta for BAV patients, which will help to discover the hemodynamic factors including the development of ascending aorta and provide more information and further understanding of this BAV complication.

Results

In order to describe the results intuitively, five feature moments were selected from one cardiac cycle of the velocity waveform of the aortic inlet, which were the early systolic phase (t=0.10s), the maximum inlet velocity phase (t=0.17s), the late systolic phase (t=0.29s), the maximum regurgitation phase (t=0.43s) and stable diastolic phase(t=0.51s), respectively.

Flow velocity, patterns and ratio

Fig.3 shows the flow pattern within the aorta at the systolic peak and the late systolic phase. The aorta entrance area is reduced by bicuspid aortic valve malformation,

so when the blood flows into the aortic sinus at the systolic peak, the velocity is high, which is up to 2.2m/s. It was an important observation when you compare this velocity with the normal aortic entrance velocity (1.0-1.7m/s)(6). However, the velocity of blood flow drops abruptly when flowing past the AAo and form a large regurgitation, which makes the blood flow disorder. At the late systolic phase, the turbulent blood flow rushes at the outer of the AAo wall. When the AAo is dilated to the diameter of 5cm, the maximum velocity is higher than that of the other three and the area of wall affected by the relatively high flow is larger as well. In order to better observe the blood flow velocity, the velocity profile of the sinotubular junction and the proximal AAo were analyzed, as shown in Fig.4a, 4b.

At systolic peak (Fig.4a at 0.17s), there is no significant difference in velocity among four models when the flow past the sinotubular junction. The velocity is higher in central blood flow and the flow velocity is lower near the wall of the vessel. There is a low blood flow velocity in the periphery of the central region. However, the velocity contours of the proximal AAo presented in Fig.4b at 0.17s are somewhat different: a. the area within high velocity (velocity>1.6m/s, orange and red area) increased with the increasing diameter of the vessel; b. when the AAo is dilated to the diameter of 5cm, the maximum velocity is obviously higher than that of the other three; c. the high flow rate area is shifted to the left. Comparison among the four different ascending aortic configurations highlights that the flow is characterized by a greater asymmetry with the increase in diameter.

Pressure

The largest pressure difference (based on the ascending aortic inlet pressure) occurs at systolic peak, with the highest blood flow velocity. The pressure difference from aortic annulus to AAo is depicted in Fig. 5. The pressure at the proximal of AAo is high and decreases from the proximal to the distal end gradually. However, as the AAo diameter increases, the pressure in AAo increases correspondingly. The other main characteristic of pressure distribution is its asymmetry. The pressure at the outer wall is lower than that in the other inner regions of AAo.

wall shear stress distributions

Fig. 6a displays wall shear stress contours at five featured moments. At systolic peak(t=0.17s), and flow is most furious when entering the valve, the proximal AAo wall shear stress(WSS) is much higher than that in other regions. The WSS distributions at the late systolic phase(t=0.29s) and the maximum regurgitation phase(t=0.43s) in all of the cases are above 10Pa around the mid-ascending aorta, especially for the case with 5cm diameter. Additionally, when t=0.29s, the maximum WSS values of M1, M2, M3 and M4 are 24Pa, 27Pa, 28pa and 31Pa, respectively. At the early systolic phase(t=0.10s) and stable diastolic phase(t=0.51s), WSS values of the both sides are stable without obvious changes, for all cases.

However, a better representative of WSS is time averaged wall shear stress (TA WSS), which is obtained by averaging the WSS in a cardiac cycle. From the TAWSS distribution trends(Fig. 6b), the four models are basically the same, but the area around the distal of AAo partially appears high TAWSS, and TAWSS is higher when AAo diameter is larger.

As for OSI in Fig. 7, for the outer part, the statistical results of area-averaged OSI on the proximal AAo wall increase with the increase of the diameter. For the inner part, it is a constant almost. Moreover, it is apparent to see the OSI values of the outer becomes greater than that of the inner in M4 with 5cm diameter.

Hemodynamic parameter distribution of the AAo is quite asymmetric, especially for M4 : 1.speed: with the dilation degree increases, the flow velocity increases, and the higher velocity region shifts to the outside; 2.The pressure of the outer is lower than that in the other regions of AAo, and it gradually increases with the increase of the dilatation degree; 3.WSS: When the case with 5cm diameter, especially at the late systolic phase and the maximum regurgitation phase, WSS is much higher than that of others; 4.OSI: the OSI of the outer has a gradual increase as the diameter increases.

Discussion

To expand the understanding of ascending aorta dilation for BAV patients, the hemodynamic environments in the ascending aorta at different development stages of

dilation were numerically investigated. The results revealed that BAV patients with valvular dilation have altered flow patterns, pressure difference, WSS and OSI distribution features, and more parts of aorta would be affected with the increasing ascending aorta diameters.

BAV after the aortic root dilation formed is associated with eccentric turbulent flow through the bicuspid valve and asymmetrically increased wall stress on the aortic wall, which leads to subsequent aortopathy. The flow jet directed toward the wall of the proximal AAo, and the local pressure induced by turbulence of blood flow is an important determinant of vascular enlargement, aneurysm growth and rupture. Besides, elevated OSI levels are accompanied by low WSS, and together they serve as indicators for vascular injury. In addition, the asymmetrically distributed WSS, eccentric systolic blood flow and the pressure distribution asymmetry of the proximal AAo wall increase haemodynamics burden which is also a risk for aneurysm formation in the AAo(5). Besides, the appearance of vortex and the slowing blood flow in the proximal AAo provide the pathogenic substance such as lipids to interact with the arterial wall with a longer time, leading to more infiltration of these harmful mediators into the vessel wall.These hemodynamic parameters alternations are likely to lead to consecutive aortic wall remodeling, which gradually results in the expansion of the arterial vessels, and make the aorta wall thinner, the wall tension increased and vascular stiffness and elasticity decreased. Factually, from these four BAV models with the aortic sinus expanded, we could see a process in which AAo expands continually and hemodynamic abnormality has added significant.

More parts of aorta would be affected with the increasing ascending aorta diameters in BAV patients after dilation formed. The velocity contours of the proximal AAo at systolic peak showed that the area of high velocity (velocity>1.6m/s, orange and red area) increased with the increasing diameter of the vessel, as well as the area of high pressure(pressure>1000pa, red area) in AAo, especially in the distal side of the AAo. As for TAWSS, the area around brachiocephalic artery displays partially high when the AAo is more than 4.5 cm in diameter. This point is of great value in the process of making reference for disease progression and the choices of surgical extent

to BAV. For BAV anatomy, considering the association of valve dysfunction and aortic dilatation or its complications, a group of affected individuals will require combined treatment of aorta and aortic valve.

When an individual is referred for surgery, medical decision to resect aortic tissues in BAV aortopathy is difficult, because the degree of aortic dilatation can be highly variable with respect to location on the aorta and the degree of enlargement. and potential hemodynamic effects on aortic arch with the increasing ascending aorta diameters in BAV patients after dilation formed would be a part that cannot be ignored for the treatment of adults with bicuspid aortopathy. Based on recent studies (11), AHA/ACC Guidelines (12) provide some recommendations: operative intervention to repair or replace the aortic root (sinuses) or replace the ascending aorta is indicated (Class I) in asymptomatic patients with BAV if the diameter of the aortic root or ascending aorta is 5.5 cm or greater; operative intervention to repair or replace the aortic root (sinuses) or replace the ascending aorta is reasonable (Class II) in asymptomatic patients with BAV if the diameter of the aortic root or ascending aorta is 5.0 cm or greater and an additional risk factor for dissection is present (e.g. family history of aortic dissection or aortic growth rate 0.5 cm per year) or if the patient is at low surgical risk and the surgery is performed by an experienced aortic surgical team in a center with established expertise in these procedures; replacement of the ascending aorta is reasonable (Class II) in BAV patients undergoing aortic valve replacement(AVR) because of severe aortic stenosis or aortic regurgitation when the diameter of the ascending aorta is greater than 4.5 cm. Besides, there is another distinct evaluation system (13, 14) including 4 patterns of aortic dilatation in patients with bicuspid aortic valves. Patients in clusters III (tubular portion and transverse arch) and IV (aortic root and tubular portion with tapering across the transverse arch) should have transverse arch replacement (plus concomitant root replacement in cluster IV). Patients in cluster I (aortic root alone) should undergo complete aortic root replacement, whereas in patients in cluster II (tubular ascending aorta alone) supracommissural ascending aortic grafting is adequate. The above two suggestions are not well implemented in clinical practice actually, because it’s impossible to enumerate all the cases in a

recommendation, and each patient will be given an individualized evaluation according to patient's age, complications and shape of AAo etc. and anticipated risks of operation must be weighed against the risks of dissection and rupture.

Limitations

While it must be mentioned that, the findings of the present study are limited by some of the assumptions involves. The original computational model was carried out using original data derived from only one representative patient with BAV and aortic aneurysm. Future studies can enlarge the sample size, and add BAV valve classification for comparative analysis. Another limitation is that the blood vessel elasticity, the wall motion and fluid-solid interaction were not involved in all the simulations in this study. In comparison with the simulation involving structure part, this assumption may affect the accuracy of the results slightly, but it is acceptable.

Conclusion

This study focuses on hemodynamic of BAV models with different AAo dilation levels by numerical simulation. BAV patients with valvular dilation have altered flow patterns, pressure difference, WSS and OSI distribution features, and more parts of aorta would be affected with the increasing ascending aorta diameters. According to the results of the numerical simulation, when AAo diameter exceeds 5.0cm, hemodynamic abnormity is more obvious and it would be actively considered to replace aortic root, the ascending aorta and aortic arch. Therefore, more attention should be paid for BAV group.

In patients with BAV and ascending aortic dilatation, we could use CFD numerical simulation to make an assessment and find the hemodynamics in patients with abnormal point to predict disease progression timely. This could provide hemodynamic basis for surgery in the future. It will help to study the disease mechanism, timing of surgery, and determination of surgical options.

Methods

Patient

This study was approved by local ethics committee (2016047X, Beijing Anzhen Hospital, Capital Medical University). A total of 14 patients with BAV were retrieved

from the hospital information management system from June 1 to September 1, 2016, of which 6 patients had BAV with ascending aorta dilatation. This patient is male, 51 years old, whose information was collected on August 3, 2016 in Anzhen hospital. Patients were screened by Echocardiography, the aortic valve is BAV with left/right cusp fusion as well as mild-stenosis; ascending aortic was dilatation, which diameter was 5.2cm. The patient confirm he don`t have any past medical history such as hypertension, hyperlipidemia, coarctation of aorta, aortic dissection and marfan syndrome.

Numerical model of the aorta

The numerical model of the aorta was established based on the MRI data (in-plane resolution of 512 by 512 pixels with a pixel size of 0.7 mm and slice thickness of 1.25 mm, total 600 images). This MRI was used for the Trio Tim 3.0 T MRI scanner of Siemens of Germany, with the maximum switching rate of 200 T/(m · ms) and the maximum gradient strength of 45mt/m. The phase-controlled front ring, the heart gate control scan. Image segmentation and surface reconstruction of BAV were accomplished by a semi-automatic threshold-based segmentation tool (Mimics17.0, Materialise Inc., Belgium).

After smoothed, the format of aorta model was saved as X_T format (a kind of parasolid model file format) from stereolithography by extracting surface function (Geomagic Wrap2015, Geomagic Inc., USA). Starting from the sinotubular junction to the end of AAo, aorta model was cut off and we got two sections. The profile of the cross-section at the maximum diameter of the AAo is traced, and the diameter of the cross-section was set to 3.5cm, 4.0cm, 4.5cm and 5.0cm, respectively. Along the aorta axis, lofting was made by contours of three sections by CAD (Computer Aided Design) tool (SolidWorks2015, SolidWorks Inc., France). The final four models named Model1, Model2, Model 3 and Model 4 (M1, M2, M3 and M4) are shown in **Fig.1**.

Meshing

A semi-automatic adaptive meshing technique was employed in HyperMeshv10.0 (Altair HyperWorks, Troy, MI, USA) to optimize both computational efficiency and element quality. 4-noded tetrahedral elements were assigned to all models, and element

size was set to 0.0014m and 5 boundary layers near the walls. The grid was divided into various entrance, exits and the inner/outer of AAo regions. The number of elements and nodes of models meshed as are shown in **Table 1**.

Boundary conditions and flow models

Transient analysis was adopted to investigate the pulsatility of blood flow. No-slip boundary conditions were assigned at the wall in all cases. The numerical simulation was based on the three dimensional incompressible Navier-Stokes equations and continuity equations:

$$\rho\left(\frac{\partial U}{\partial t}\right) + (U - U_m) \cdot \nabla U = -\nabla p + \nabla \cdot \tau \quad (1)$$

$$\nabla \cdot \vec{u} = 0 \quad (2)$$

Where $\vec{u}$ and *p* respectively represent the fluid velocity vector and the pressure. ρ and μ are the density and viscosity of blood, and τ is stress tensor. It was treated that blood is incompressible, and blood has same kinematic viscosity and density(15, 16) of Newtonian fluid with a dynamic viscosity of 3.5 m·Pa and a density of 1050 kg/m^3.

Time-varying velocity profile was imposed at the inlet of the aorta, based on the flow velocity waveforms that had been obtained from the in vivo measurements. The flow rates entering the brachiocephalic, left common carotid, and left subclavian arteries were specified to be 12%, 5% and 8%(17, 18) of the blood flow rate entering the aortic root, respectively.

The maximum Reynolds numbers(Re_{max}) in our models is 2445, and the average Reynolds numbers (Re_{ave}) based on the average flow velocity (V_{ave}) at peak systole is 1149. The Womersley numbers(α) is 22.5 and the blood flow is assumed to be laminar. The calculation time step and cardiac cycle were set to 0.01s and 0.8s, respectively. To minimize the influence of initial flow conditions, all simulations were carried out by a commercial finite-volume-based CFD solver (Fluent14.5, ANSYS, Inc., USA) for six cardiac cycles to achieve a periodic solution, and the results presented here were obtained in the sixth cycle.

Derived Haemodynamic Parameters

Derived haemodynamic wall parameters include the velocity, pressure, WSS, and oscillatory shear index (OSI). WSS is an analytical factor used to describe the dynamic friction between the viscous fluid and the solid wall, which is caused by the lateral movement of the viscous fluid. The time-averaged wall shear stress (TAWSS) is obtained by averaging the WSS in a cardiac cycle and is a better representative of WSS.

$$TAWSS = \frac{1}{T}\int_0^T WSS\,dt \tag{3}$$

OSI reflects the cyclic departure of the WSS (or velocity) vector from predominant direction of blood flow and is calculated as equation (4):

$$OSI = \frac{1}{2}\left(1 - \frac{\left|\int_0^T \tau_\omega dt\right|}{\int_0^T \left|\tau_\omega\right| dt}\right) \tag{4}$$

where τ_ω is wall shear stress and T is one cardiac cycle. The OSI values vary from 0 to 0.5: 0 represents unidirectional flow, and 0.5 signifies complete oscillatory flow.

List of Abbreviations

BAV, bicuspid aortic valve; AAo, the ascending aortic; CFD, computational fluid dynamics; WSS, wall shear stress; OSI, oscillatory shear index; CAD, computer aided design; TAWSS, time-averaged wall shear stress

Declarations

Ethics approval and consent to participate

Written informed consent was obtained from the subject for the publication of this study and any accompanying, in accordance with the regulations of the local ethics committee (2016047X, Beijing Anzhen Hospital, Capital Medical University).

Consent for publication

Consent for publication was obtained for the patient's data included in the study.

Availability of data and materials

The datasets used and analyzed during the current study are available from the corresponding author on reasonable request, and most data generated or analyzed during this study are included in this published article and its supplementary information files.

Competing interests

The authors declare that they have no competing interests.

Funding

This work was supported by the Research and demonstration application of clinical diagnosis and treatment technology from Beijing Municipal Science and Commission （Z19110700660000）. National Science Foundation of China (81970393) and the National Key Technology R&D Program (No. 2015BAI12B03), and Beijing Major Science and Technology Projects from Beijing Municipal Science and Technology Commission(Z171100001017083).

Author contributions

T.Z. and S.Z. researched data and participated in writing of the manuscript. J.M.Z. performed the experiments, J.F.O. and S.J.L. contributed to the discussion. T.Z., J.M.Z. provided oversight for the project and participated in editing of the manuscript.

Acknowledgements

The authors appreciate Anqiang Sun(Ph.D. & Associate Professor) and Minjia Zhu (M.S.) who are members of the Key Laboratory for Biomechanics and Mechanobiology of Ministry of Education, School of Biological Science and Medical Engineering, Beihang University.

Reference

1. Siu SC, Silversides CK. Bicuspid aortic valve disease. J Am Coll Cardiol. 2010;55(25):2789-800.
2. Meierhofer C, Schneider EP, Lyko C, Hutter A, Martinoff S, Markl M, et al. Wall shear stress and flow patterns in the ascending aorta in patients with bicuspid aortic valves differ significantly from tricuspid aortic valves: a prospective study. Eur Heart J Cardiovasc Imaging. 2013;14(8):797-804.
3. Bonomi D, Vergara C, Faggiano E, Stevanella M, Conti C, Redaelli A, et al. Influence of the aortic valve leaflets on the fluid-dynamics in aorta in presence of a normally functioning bicuspid valve. Biomech Model Mechanobiol. 2015;14(6):1349-61.
4. Cao K, Atkins SK, McNally A, Liu J, Sucosky P. Simulations of morphotype-dependent hemodynamics in non-dilated bicuspid aortic valve aortas. J Biomech. 2017;50:63-70.
5. Barker AJ, Markl M, Burk J, Lorenz R, Bock J, Bauer S, et al. Bicuspid aortic valve is associated with altered wall shear stress in the ascending aorta. Circ Cardiovasc Imaging. 2012;5(4):457-66.
6. Nkomo VT, Enriquez-Sarano M, Ammash NM, Melton LJ, 3rd, Bailey KR, Desjardins V, et al. Bicuspid aortic valve associated with aortic dilatation: a community-based study. Arterioscler Thromb Vasc Biol. 2003;23(2):351-6.
7. Tadros TM, Klein MD, Shapira OM. Ascending aortic dilatation associated with bicuspid aortic valve: pathophysiology, molecular biology, and clinical implications. Circulation. 2009;119(6):880-90.
8. den Reijer PM, Sallee D, 3rd, van der Velden P, Zaaijer ER, Parks WJ, Ramamurthy S, et al. Hemodynamic predictors of aortic dilatation in bicuspid aortic valve by velocity-encoded cardiovascular magnetic resonance. J Cardiovasc Magn Reson. 2010;12:4.
9. Hahn RT, Roman MJ, Mogtader AH, Devereux RB. Association of aortic dilation with regurgitant, stenotic and functionally normal bicuspid aortic valves. Journal of the American College of Cardiology. 1992;19(2):283-8.
10. Michelena HI, Khanna AD, Mahoney D, Margaryan E, Topilsky Y, Suri RM, et al. Incidence of aortic complications in patients with bicuspid aortic valves. JAMA. 2011;306(10):1104-12.
11. Bentall H, De Bono A. A technique for complete replacement of the ascending aorta. Thorax. 1968;23(4):338-9.
12. Accf/Aha/Aats/Acr/Asa/Sca/Scai/Sir/Sts/Svm Guidelines For The D, Management Of Patients With Thoracic Aortic Disease Representative M, Hiratzka LF, Creager MA, Isselbacher EM, Svensson LG, et al. Surgery for Aortic Dilatation in Patients With Bicuspid Aortic Valves: A Statement of Clarification From the American College of Cardiology/American Heart Association Task Force on Clinical Practice Guidelines. Circulation. 2016;133(7):680-6.
13. Verma S, Siu SC. Aortic dilatation in patients with bicuspid aortic valve. N Engl J Med. 2014;370(20):1920-9.

14. Fazel SS, Mallidi HR, Lee RS, Sheehan MP, Liang D, Fleischman D, et al. The aortopathy of bicuspid aortic valve disease has distinctive patterns and usually involves the transverse aortic arch. J Thorac Cardiovasc Surg. 2008;135(4):901-7, 7.e1-2.
15. Poinsot TJ, Lelef SK. Boundary conditions for direct simulations of compressible viscous flows. Journal of Computational Physics. 1992;101(1):104-29.
16. Taylor CA, Hughes TJ, Zarins CK. Finite element modeling of three-dimensional pulsatile flow in the abdominal aorta: relevance to atherosclerosis. Ann Biomed Eng. 1998;26(6):975-87.
17. Feintuch A, Ruengsakulrach P, Lin A, Zhang J, Zhou YQ, Bishop J, et al. Hemodynamics in the mouse aortic arch as assessed by MRI, ultrasound, and numerical modeling. Am J Physiol Heart Circ Physiol. 2007;292(2):H884-92.
18. van der Giessen AG, Groen HC, Doriot PA, de Feyter PJ, van der Steen AF, van de Vosse FN, et al. The influence of boundary conditions on wall shear stress distribution in patients specific coronary trees. J Biomech. 2011;44(6):1089-95.

Figure legends

Fig.1 Four numerical models of BAV numerical models were established. (a)The diameters of the ascending aorta (AAo) are 3.5cm, 4.0cm, 4.5cm and 5.0cm, respectively; while, the size and the appearance of other parts are fixed. The aortamitral valve area is 292.2mm^2, and the diameter of the valsalva sinus is 5.18cm; (b)Regions of interest where the hemodynamic were analyzed.

Fig.2 The cross-sectional velocity profile of the inlet at the ascending aorta. The data is obtained from in vivo measurements.

Fig.3 Flow pattern within the AAo analysis at systolic peak by drawing lines that are tangential to the instantaneous velocity vectors. These lines are contoured by velocity magnitude.

Fig.4 Vector contours of two sections at systolic peak. The (a) and (b) display the flow pattern of sinotubular junction (plane 1) and the proximal AAo (plane 2), respectively. The left side of contours is the outer and the right side is the inner.

Fig.5 displays the pressure difference distributions of the four models with different diameters, respectively.

Fig.6 displays the WSS distributions of the four models with different diameters at five feature moments.

Fig.7 The histogram displays oscillatory shear index(OSI) average value of the inner (the blue color column) and outer (the red color column), and it shows the difference of average OSI value between the inner and outer.

Tables

Table 1 - The numbers of elements and nodes of each model.

	M1	M2	M3	M4
Elements	778406	822982	866242	915330
nodes	212904	222098	231944	241901

Figures

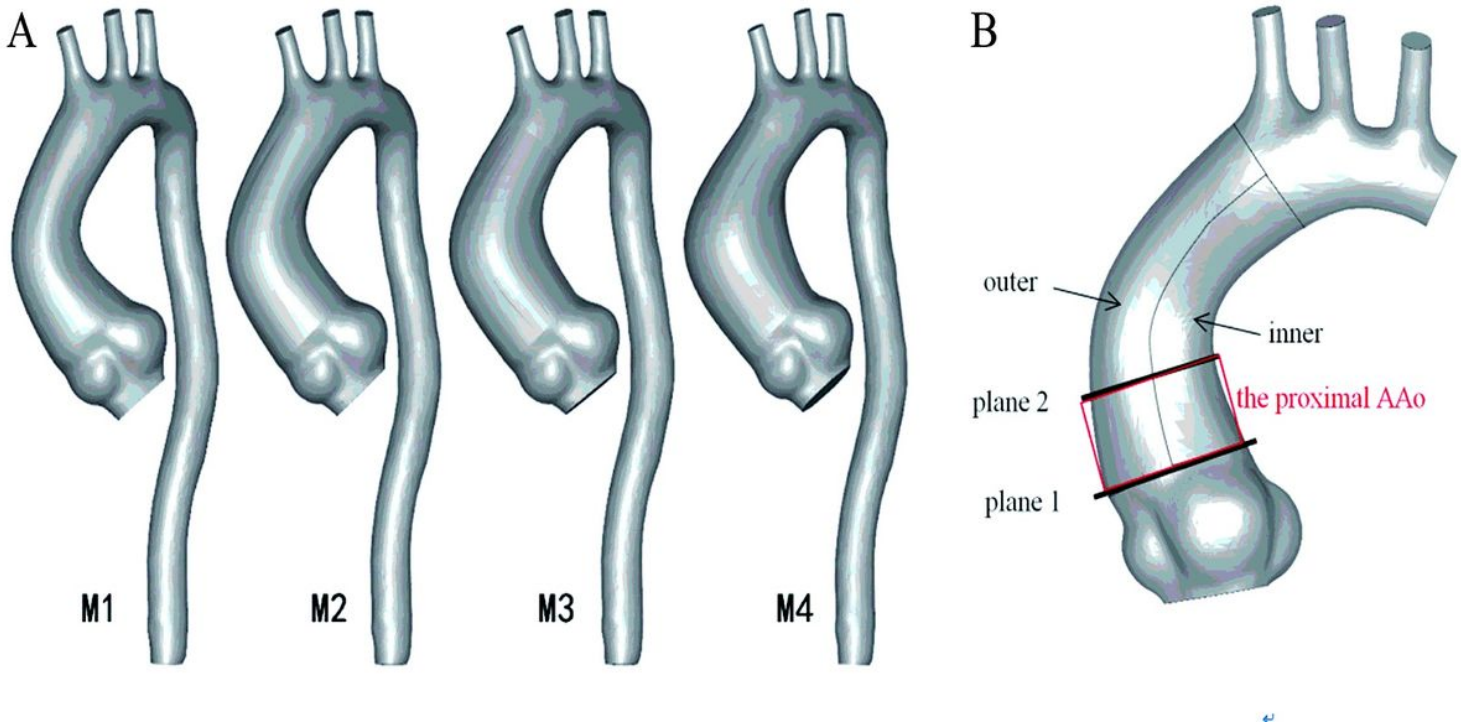

Figure 1

Four numerical models of BAV numerical models were established. (a)The diameters of the ascending aorta (AAo) are 3.5cm, 4.0cm, 4.5cm and 5.0cm, respectively; while, the size and the appearance of other parts are fixed. The aortamitral valve area is 292.2mm2, and the diameter of the valsalva sinus is 5.18cm; (b)Regions of interest where the hemodynamic were analyzed.

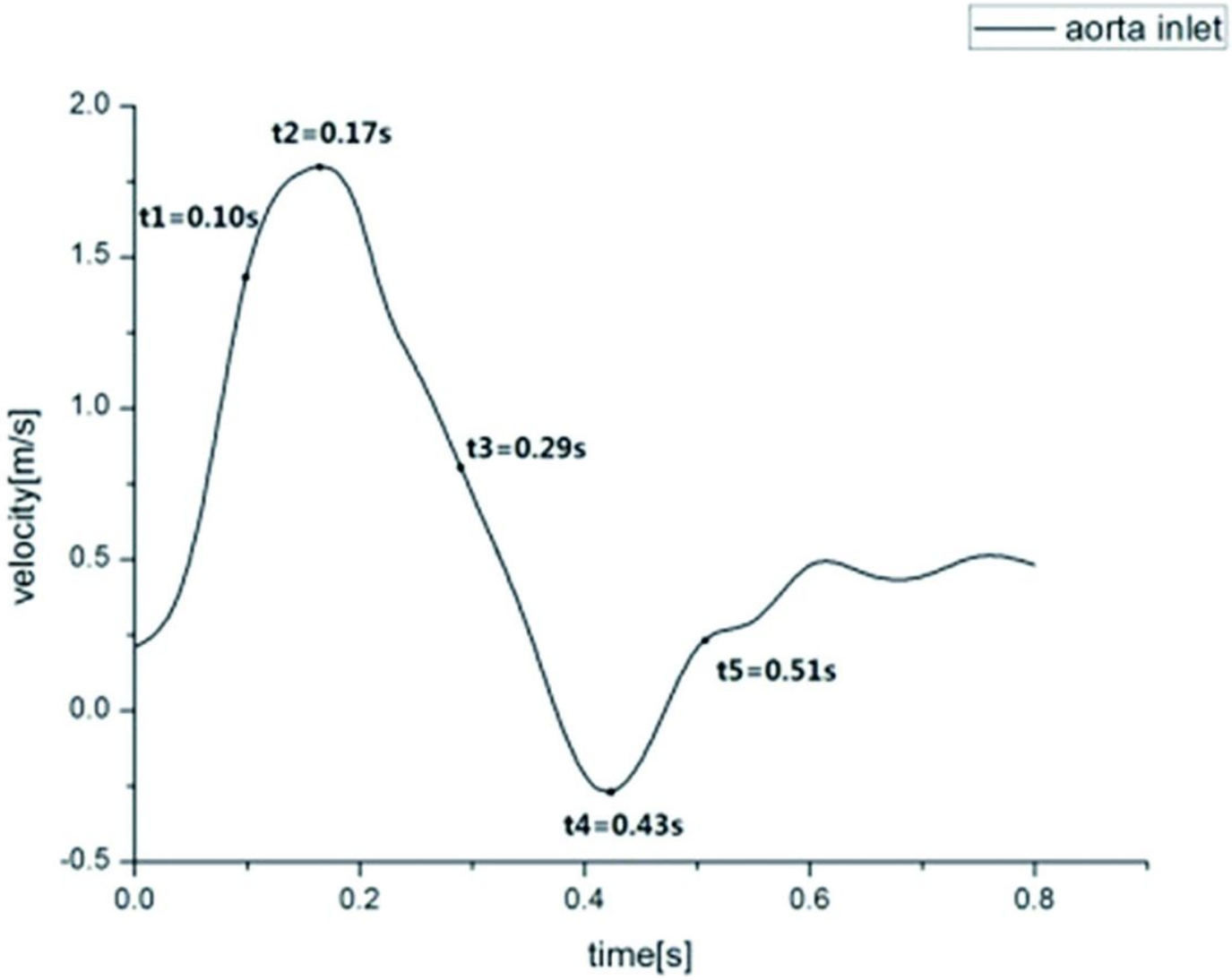

Figure 2

The cross-sectional velocity profile of the inlet at the ascending aorta. The data is obtained from in vivo measurements.

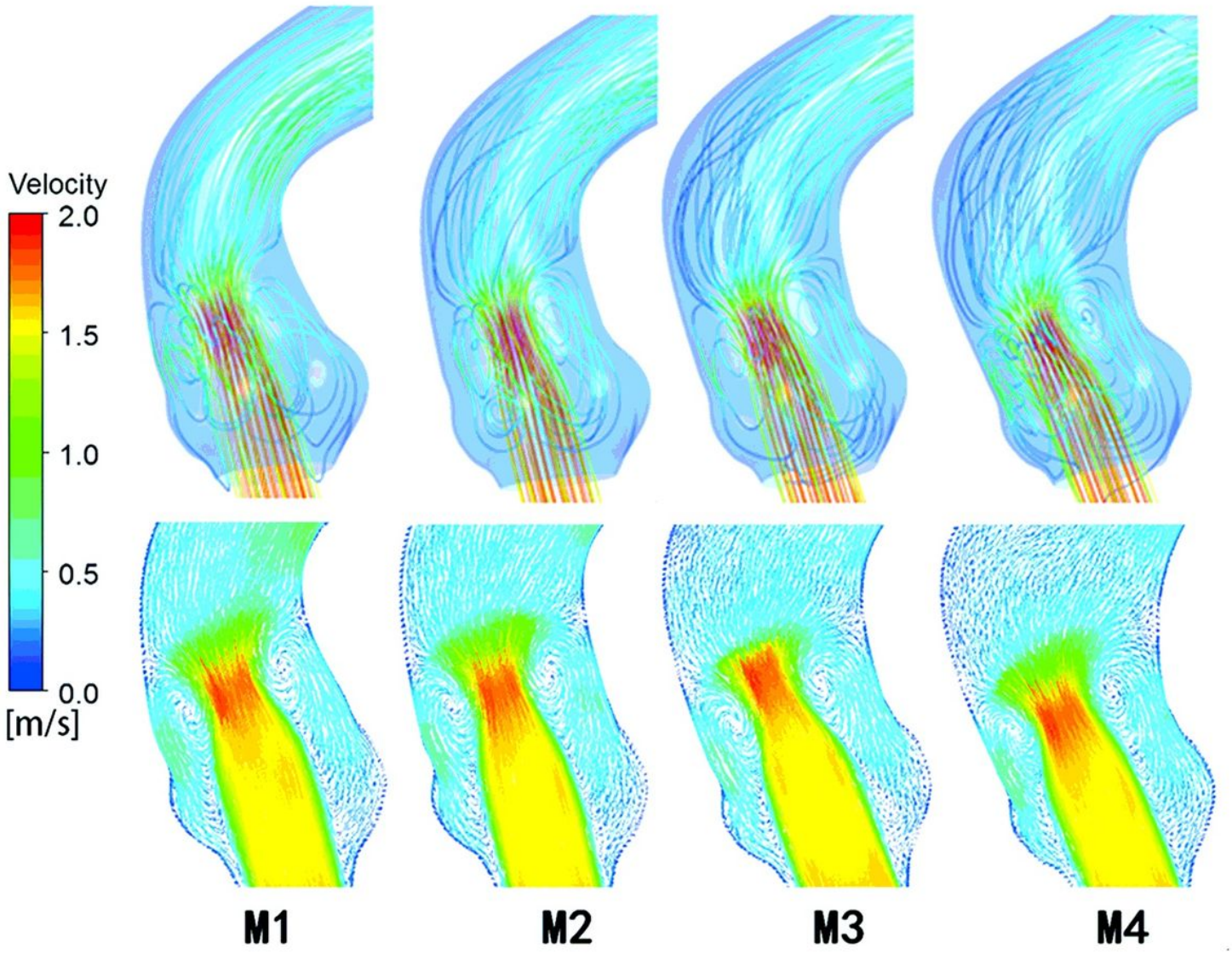

Figure 3

Flow pattern within the AAo analysis at systolic peak by drawing lines that are tangential to the instantaneous velocity vectors. These lines are contoured by velocity magnitude.

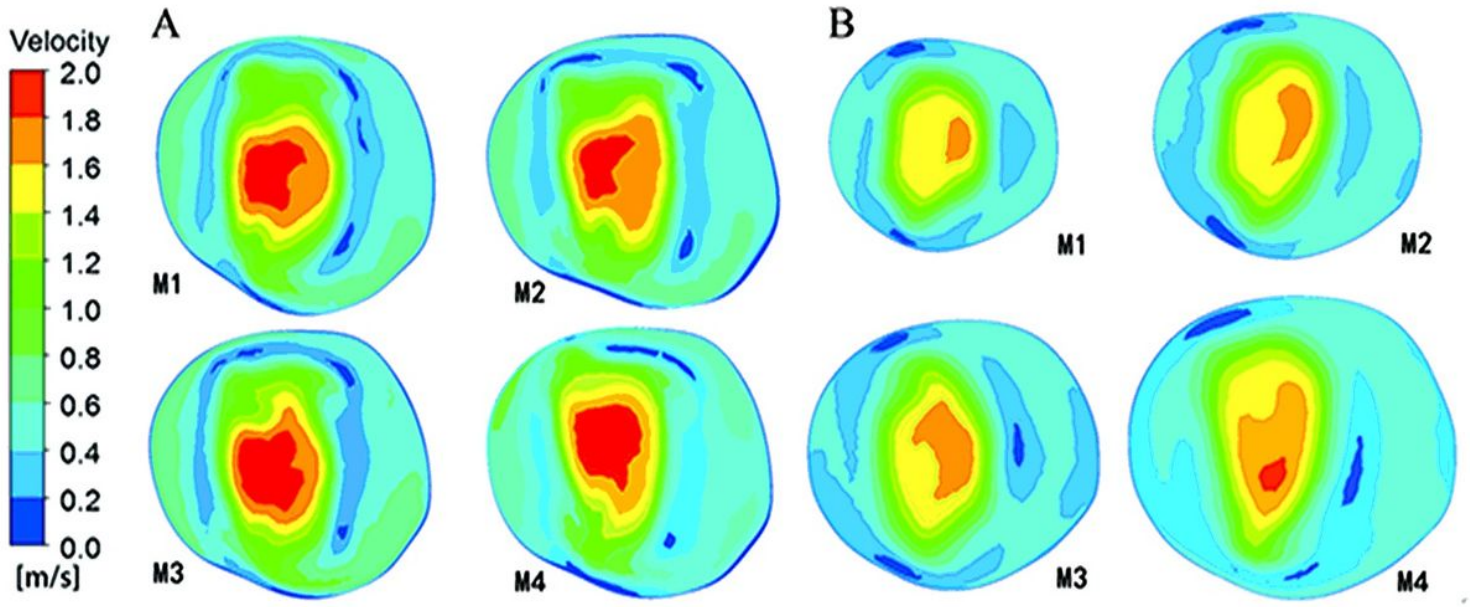

Figure 4

Vector contours of two sections at systolic peak. The (a) and (b) display the flow pattern of sinotubular junction (plane 1) and the proximal AAo (plane 2), respectively. The left side of contours is the outer and the right side is the inner.

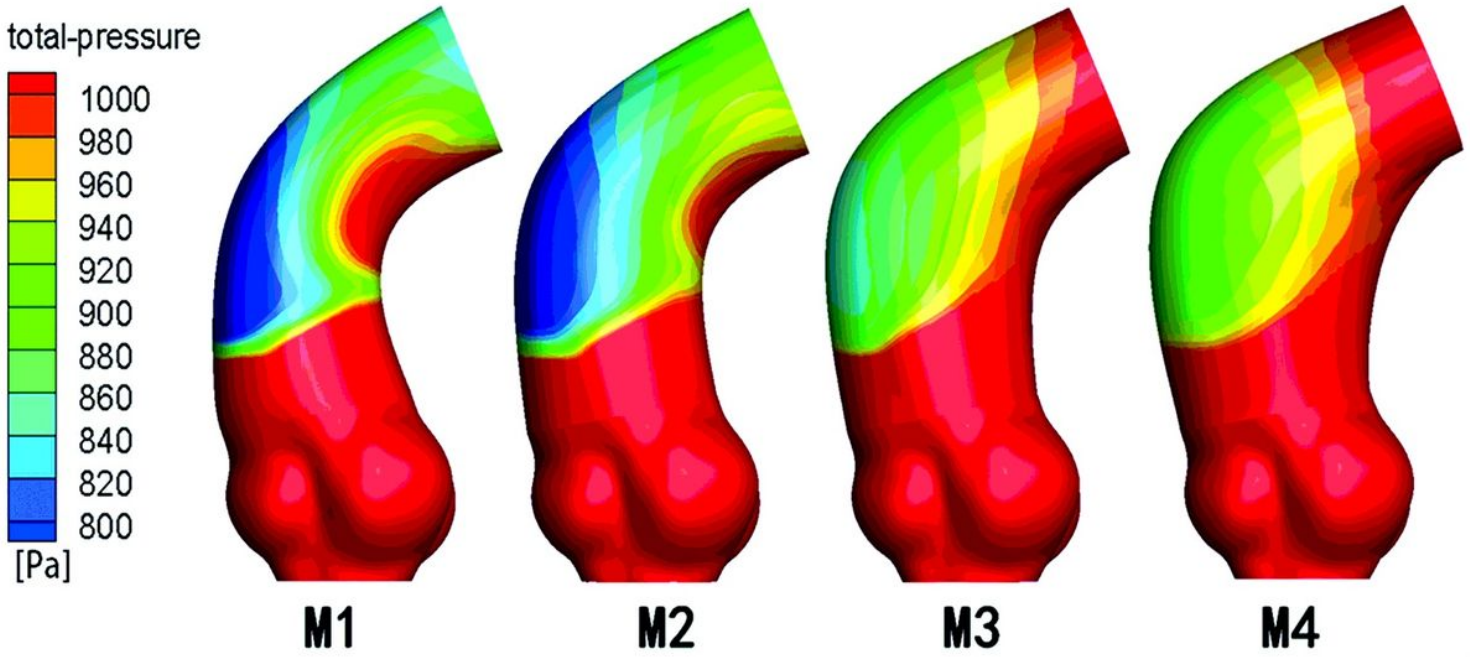

Figure 5

displays the pressure difference distributions of the four models with different diameters, respectively.

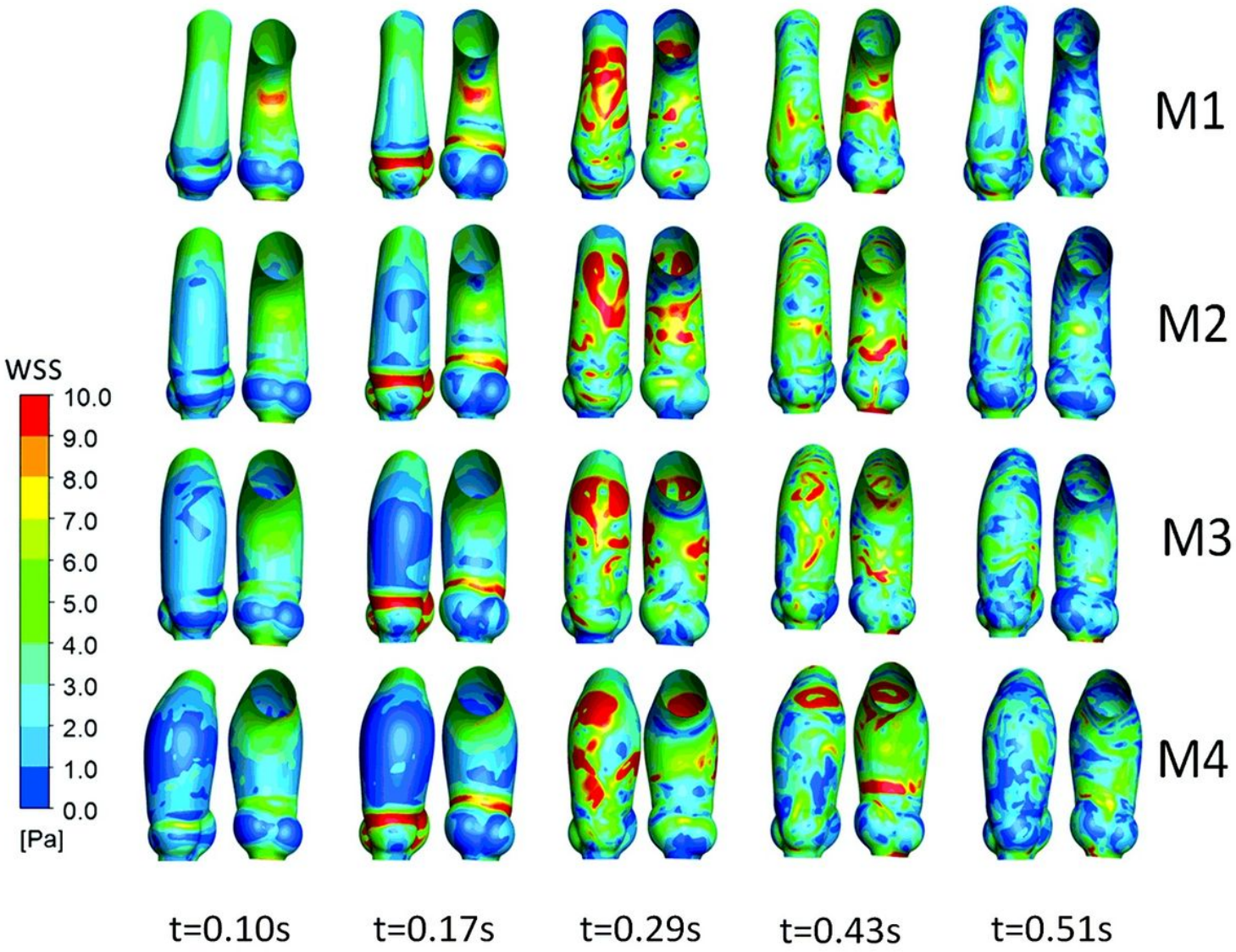

Figure 6

displays the WSS distributions of the four models with different diameters at five feature moments.

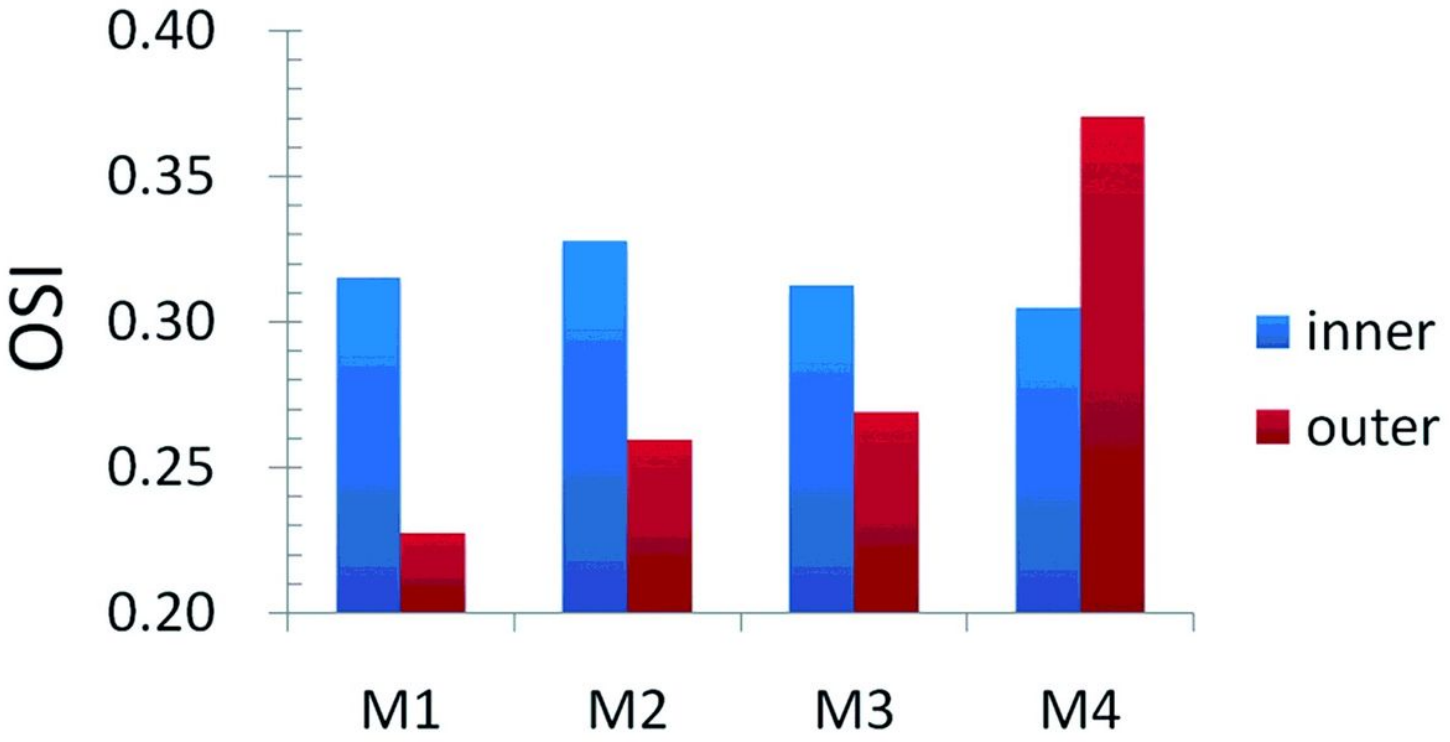

Figure 7

The histogram displays oscillatory shear index(OSI) average value of the inner (the blue color column) and outer (the red color column), and it shows the difference of average OSI value between the inner and outer.

Supplementary Files

This is a list of supplementary files associated with this preprint. Click to download.

- 12.mp4
- 11.mp4
- 10.mp4
- 9.mp4
- 8.mp4
- 7.mp4
- 6.mp4
- 5.mp4
- 4.mp4
- 3.mp4
- 2.mp4

- 1.mp4